



3-Hydroxybenzo[g]quinolones: dyes with red-shifted absorption and highly resolved dual emission

Mykhailo D. Bilokin^{a,*}, Volodymyr V. Shvadchak^{a,b}, Dmytro A. Yushchenko^{a,b}, Andrey S. Klymchenko^b, Guy Duportail^b, Yves Mely^b, Vasyl G. Pivovarenko^{a,b,*}

^a Department of Chemistry, National Taras Shevchenko University of Kyiv, 01601 Kyiv, Ukraine

^b Laboratoire Biophotonique et Pharmacologie, UMR 7213 du CNRS, Université de Strasbourg, Faculté de Pharmacie, 74 route du Rhin, 67401 Illkirch, France

ARTICLE INFO

Article history:

Received 16 April 2009

Revised 31 May 2009

Accepted 3 June 2009

Available online 9 June 2009

Keywords:

Fluorescent sensors

Ratiometric probes

Intramolecular proton transfer

ESIPT

3-Hydroxyquinolones

Solvent basicity

Hydrogen-bond acceptor ability

ABSTRACT

New derivatives of 3-hydroxyquinolone (3HQ) with a fused benzene ring (3-hydroxybenzo[g]quinolones) have been synthesized. They display a remarkable red shift of their absorption spectrum in comparison with other 3HQ analogs allowing their excitation by common He/Cd and Ar-ion lasers. As a result of their irreversible excited-state intramolecular proton transfer (ESIPT) reaction, they display a dual fluorescence in a series of solvents of varying polarities, starting from toluene to methanol. The dual emission of these dyes correlates well with solvent H-bond basicity, which is connected with the effect of this solvent property on the kinetics of the ESIPT reaction. In addition to their red-shifted absorption and fluorescence, these new derivatives show a larger separation of their two emission bands and a more appropriate range of their intensity ratio than the previously synthesized 3HQs. These properties allow an improved ratiometric evaluation of the local H-bond basicity of unknown environments, which will favor future applications of the new dyes in polymer and biological sciences.

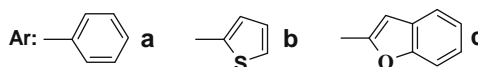
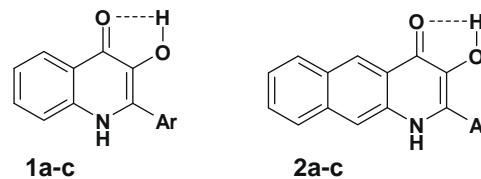
© 2009 Elsevier Ltd. All rights reserved.

1. Introduction

Fluorescence methods are powerful tools for investigating biomolecular interactions.¹ There is notably a strong demand for the development of new fluorescent probes that could sense the electric fields as well as the H-bond donor and H-bond acceptor abilities in protein binding sites. In this respect, probes with a dual emission (two-channel emitters) present the strong advantage over intensimetric probes (single-channel emitters) to give a ratiometric response independent of the probe concentration. Excited state intramolecular proton transfer (ESIPT)^{2–4} is a very effective approach for the design of probes with dual fluorescence. The ESIPT reaction leads to the formation of two tautomers (normal N* and tautomeric T* forms) in the excited state of the probe, which exhibit highly separated emission bands. The most interesting representatives of ESIPT probes are 3-hydroxyflavones and their derivatives (3HF),^{5,6} They have been shown to be effective tools for investigating the polarity^{6–8}, H-bond donor ability,^{8,9} electronic polarizability⁸, and electrostatic effects in different media^{10,11} including model lipid membranes,^{12–15} cell membranes^{15–17}, and proteins.^{18,19} Moreover, these dyes were shown to be useful to determine the nature and concentration of cations and anions.^{20–22}

However, despite their advantages over common single-band probes, 3HFs exhibit relatively low photostability and quantum yields in water that limit their applications. As a consequence, the development of new dual-fluorescence probes with improved fluorescent properties is strongly required.

3-Hydroxyquinolones (3HQs, **1**) are structural aza-analogs of the 3HFs that also display a well-resolved dual emission due to an ESIPT reaction.^{23–25} These recently introduced dyes present important advantages over 3HFs, since they are more photostable and exhibit higher fluorescence quantum yields in aqueous solutions.²³ 3HQ dyes were shown to be effective in sensing the viscosity of protic solvents²⁶ as well as both the polarity and basicity of organic media.^{27,28}



* Corresponding authors. Tel.: +38 044 239 33 12; fax: +38 044 220 83 91 (V.G.P.).
E-mail address: pvg_org@ukr.net (V.G. Pivovarenko).

Laser excitation sources are frequently used in biological experiments. To avoid autofluorescence and photo-degradation of the biological samples, it is important to use an excitation wavelength longer than 420 nm. Concerning dual-fluorescence probes, only few 3HF dyes can be excited by laser sources at 442 or 452 nm,²⁹ while none of the reported 3HQs exhibit significant absorbance at such wavelengths. In this respect, we present herein the synthesis and spectroscopic properties of new dyes of the 3HQ family (series **2**), which possess one additional benzene ring fused by the border [g] to the quinolone system. These dyes have been designed by considering the principle that the increase in the length of the conjugated π -electron system should lead to a red shift of the absorption band. Then, to further modulate the spectroscopic properties we introduced 2-aryl substituents of different length and electron donor ability. The new dyes exhibit superior absorption and fluorescence properties compared to their parent 3HQ analogs.

2. Results and discussion

Synthesis (Scheme 1) and purification of the 3HQ dyes **1–2** as well as their physical properties and their structural data are described in the Experimental section. The absorption and fluorescence properties of the new dyes **2a–c** (benzo-analogs) were studied and compared with those of the parent dyes **1** in protic (methanol, ethanol) and aprotic, (toluene, ethylacetate, dichloromethane, tetrahydrofuran, THF, acetonitrile, dimethylformamide, DMF, dimethylsulfoxide, DMSO) solvents of different polarity.³⁰ Data for representative solvents are given in Table 1 and Fig. 1. All benzo-analogs **2a–c** show a considerable (70–90 nm, or 3700–5000 cm^{-1}) red-shift of the absorption maximum as compared to **1a–c**. Remarkably, such red-shifted absorption makes them convenient for excitation by He/Cd and Ar-ion lasers.

This red-shift is probably due to the more extended conjugation of the benzoquinolone ring in comparison with the quinolone ring. Moreover, the red-shifted absorption of **2b** and **2c** as compared to **2a** is in line with the stronger electron donating ability of their corresponding Ar substituent and probably, with their more planar structure.²⁸ Comparison of the positions of the absorption maxima for **2a–c** in aprotic solvents (Table 1) shows that absorption of benzoquinolones is practically not sensitive to the solvent polarity. Accordingly, the blue shifts in the absorption spectra of **2a–c** in protic solvents can be ascribed to the effects of specific hydrogen bonding.

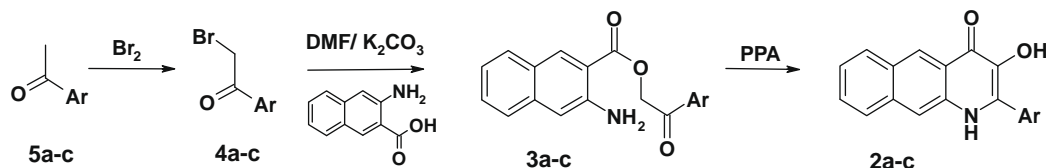
Benzo-analogs **2a–c** exhibit two bands in the emission spectra, which suggests that they undergo an ESIPT reaction, similarly to their parent analogs **1a–c**. The positions of both N* and T* emission bands in these dyes are shifted to longer wavelengths as compared to those of the corresponding parent dyes **1a–c** (Table 1, Fig. 2). The total fluorescence quantum yields for **2a–c** series are lower than for **1a–c** and do not depend on the solvent nature. The only exception is water, where their values are below 1%. For all the studied solvents, the intensity ratio of the two emission bands, I_{N^*}/I_{T^*} , in **2a–c** dyes is larger than in **1a–c**. Taking into account changes in the quantum yields, these larger values of the I_{N^*}/I_{T^*} ratio can be

ascribed both to faster non-radiative deactivation of the T* form and a slower ESIPT reaction for the dyes with the fused benzene ring. A strong effect on the I_{N^*}/I_{T^*} ratio is also observed on variation of the 2-Ar group, similarly to those observed for 3HF derivatives.³³ In both **1** and **2** series, the I_{N^*}/I_{T^*} ratio increases significantly from **a** to **c**, while the fluorescence quantum yield decreases. The observed changes in the I_{N^*}/I_{T^*} ratio on increase in the electron-donor ability of the 2-Ar group could be due to both faster non-radiative deactivation of the T* form and a slower ESIPT reaction.

Similarly to the parent analogs, dyes **2a–c** show a strong dependence of their dual emission on the solvent properties. In the polar solvent methanol, presenting high H-bond donor and acceptor abilities, the I_{N^*}/I_{T^*} ratio is much larger than in toluene, which is apolar and unable to form intermolecular H-bonds (Table 1, Fig. 3). Previously, the I_{N^*}/I_{T^*} ratio of 3HQs was shown to depend strongly on the H-bond accepting ability^{32,33} (basicity)³⁶ of solvents. Therefore, we studied in detail the correlation of the I_{N^*}/I_{T^*} ratio of the benzo-analog dye **2c** with solvent basicity for an extended range of solvents (Fig. 4). Remarkably, in contrast to 3-hydroxyflavones^{8,9} and *N*-methyl-3HQs,^{25,27} for which the I_{N^*}/I_{T^*} intensity ratio was largely governed by the solvent polarity, the I_{N^*}/I_{T^*} ratio of 3HQ-Bf did not show any regular dependency on the empirical $E_T(30)$ ³⁰ polarity parameter or the Lippert polarity or polarizability functions (Fig. 4a–c). Moreover, this ratio did not show any correlation with other solvent parameters such as the Hildebrand's solubility (Fig. 4d),³⁰ or Abraham's hydrogen bond donor acidity parameter (Fig. 4e).³¹ In contrast, the I_{N^*}/I_{T^*} ratio was found to correlate well with solvent basicity ($\log(I_{N^*}/I_{T^*}) = -1.35 + 1.71\beta$, $r^2 = 0.92$, Fig. 4f), as for the parent analog **1c**.²⁸ Taking into account that the solvent nature does not modify considerably the fluorescence quantum yield of **2a–c** dyes, the observed solvent-dependent variations of the I_{N^*}/I_{T^*} ratio are mainly due to changes in the ESIPT rate. The solvatochromic shifts for dyes **2a–c** were smaller than for dyes **1a–c**. For example, dye **1c**, which was proposed as a basicity sensor²⁸ exhibits a shift of up to 16 nm in its N*-band position in a set of 20 solvents of different polarities, while dye **2c** exhibits only a 9-nm shift for the same series of solvents (Table 1). This weaker solvatochromism suggests that dyes **2a–c** exhibit a lower difference between their S₁ and S₀ dipole moments than dyes **1a–c**.

Another important feature in the fluorescence spectra is the high separation between the two emission bands, which is about 120–150 nm (4200–4900 cm^{-1}) for all the dyes of the series **2a–c**, and reaches 160 nm (5200 cm^{-1}) for **2c** in tetrahydrofuran (Fig. 3). Such a high energy difference between the emission bands will facilitate the applications of these probes for ratiometric measurements and fluorescence microscopy imaging of biological samples.

Additional arguments on ESIPT kinetics controlling the dual emission of **2a–c** stem from the time-resolved fluorescence decays obtained for both N* and T* forms of **2a** in a series of solvents. In line with the theory of ESIPT reactions,³⁴ the fluorescence decays of both forms can be deconvoluted into fast and slow components. Moreover, the decay curve corresponding to the T* emission band contains a raising component with a negative amplitude α_1 and a



Scheme 1. Synthesis of benzo[g]quinolones **2a–c**.

Table 1
Spectroscopic properties of 3HQs and 3HBQs in solutions^a

Solvent	Ar	λ_{abs} (nm)		λ_{N^*} (nm)		λ_{T^*} (nm)		I_{N^*}/I_{T^*}		ϕ (%)	
		1	2	1	2	1	2	1	2	1	2
1. Toluene	a	371	448	419	493	505	610	0.01	0.04	38	9.7
	b	379	461	432	477	524	620	0.02	0.07	34	6.3
	c	382	468	428	493	530	633	0.06	0.22	22	4.4
2. EtOAc	a	363	447	403	478	513	611	0.03	0.11	35	8.3
	b	377	459	431	476	522	619	0.02	0.13	37	6.7
	c	383	467	438	481	527	631	0.07	0.41	25	4.1
3. CH ₂ Cl ₂	a	366	447	423	475	507	602	0.02	0.07	40	13.2
	b	377	459	434	474	516	609	0.02	0.09	50	8.5
	c	383	469	436	478	521	625	0.05	0.21	32	5.5
4. CH ₃ CN	a	362	445	424	475	510	608	0.02	0.12	32	9.0
	b	375	458	433	476	518	613	0.03	0.14	31	6.7
	c	381	466	436	479	523	625	0.09	0.47	26	4.7
5. MeOH	a	361	442	425	476	516	610	0.14	0.75	33	13.4
	b	377	452	417	481	508	607	0.16	0.94	30	9.7
	c	384	461	444	488	526	616	0.21	1.42	14	7.0

^a λ_{abs} is the position of the absorption maximum, λ_{N^*} and λ_{T^*} are the positions of the fluorescence maxima of the N* and T* forms, respectively, ϕ is the total fluorescence quantum yield.

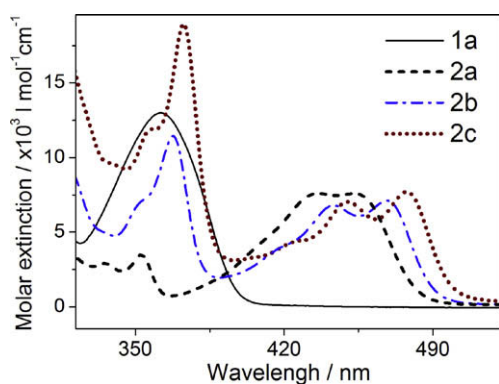


Figure 1. Absorption spectra of benzo[g]quinolones **2a–c** in methanol.

decay time corresponding to the fast emission decay component τ_1 of the N* form (Table 2), evidencing clearly that the T* excited state originates from the N* excited state through an ESIPT reaction. The long-lived decay time component τ_2 contributes greatly to the T* emission, but only marginally to the N* emission, suggesting that the ESIPT reaction is close to irreversible on the mechanism.

In the case of dye **2a**, the forward ESIPT reaction rate, which is inversely proportional to τ_1 , is about 2.5-fold slower than for **1a**,³² in line with the conclusion drawn from the comparison of their steady-state spectra. This indicates differences in the proton-transfer process between **1a** and **2a**. These differences induced by the additional benzene ring suggest a lower basicity of the carbonyl oxygen of **2a** and/or a lower acidity of the 3-OH group in the S₁ state, which could slow down the ESIPT rate reaction.³⁴

The nature of the solvent also affects strongly the ESIPT kinetics. With increasing solvent basicity in the sequence MeCN→DMF→DMSO, the fast time component τ_1 shows a gradual increase from 0.12 ns up to 2.21 ns, suggesting that the ESIPT rate decreases by more than one order of magnitude. This confirms that the dramatic increase of the I_{N^*}/I_{T^*} ratio with basicity is connected with the inhibition of the ESIPT reaction.²⁸ Thus, similarly to other 3HQs,^{32,33,37} solvents of high H-bond basicity slow down the ESIPT reaction of **2a** probably by formation of an intermolecular H-bond with its 3-OH group, which breaks the intramolecular H-bond needed for the ESIPT reaction. As a consequence, the fast component τ_1 may reflect the rate of restoration of the intramolecular hydrogen bond followed by the fast and irreversible ESIPT reaction.²⁸

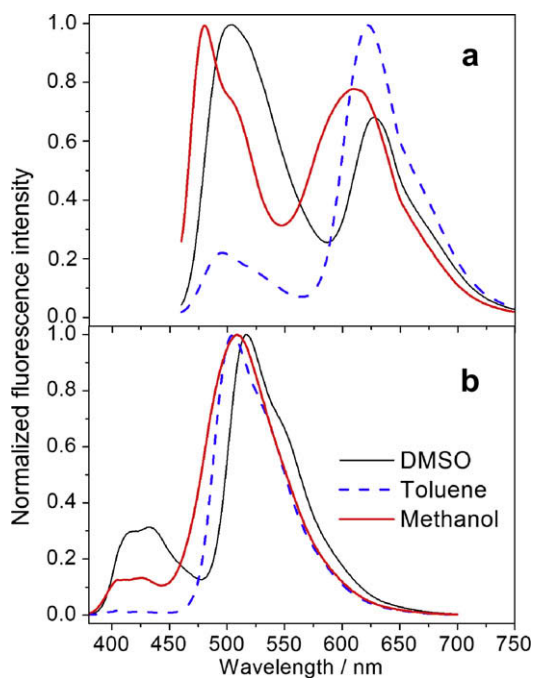


Figure 2. Normalized fluorescence spectra of quinolones **2a** (panel a) and **1a** (panel b) in organic solvents. Excitation wavelength was fixed at the absorption maximum in each case.

3. Conclusion

Three new fluorescent dyes **2a–c** were synthesized on the basis of the 3-hydroxybenzo[g]-quinolone moiety. They exhibit a red-shifted absorption band, which allows their excitation by He/Cd and Ar-ion lasers. They also display a dual fluorescence in a large set of solvents, from apolar toluene to polar methanol, due to an irreversible ESIPT reaction. The dual emission of these dyes correlates perfectly with solvent basicity (H-bond accepting ability) due to the direct effect of this property on the ESIPT kinetics. The red-shifted absorbance, the large range of the fluorescence intensity ratio I_{N^*}/I_{T^*} , and the large separation of the two emission bands of these compounds should improve the ratiometric determination of the basicity parameter of their environment, and should

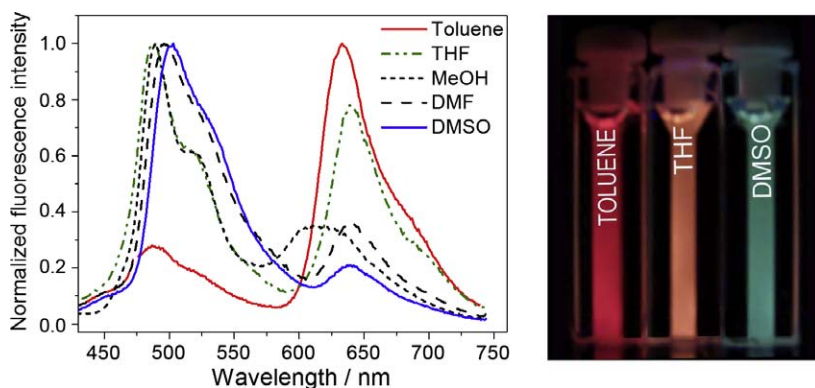


Figure 3. Normalized fluorescence spectra of **2c** in different solvents. Excitation wavelength was fixed at the absorption maximum in each case. Fluorescence of solutions of **2c** in toluene, THF, and DMSO under UV illumination.

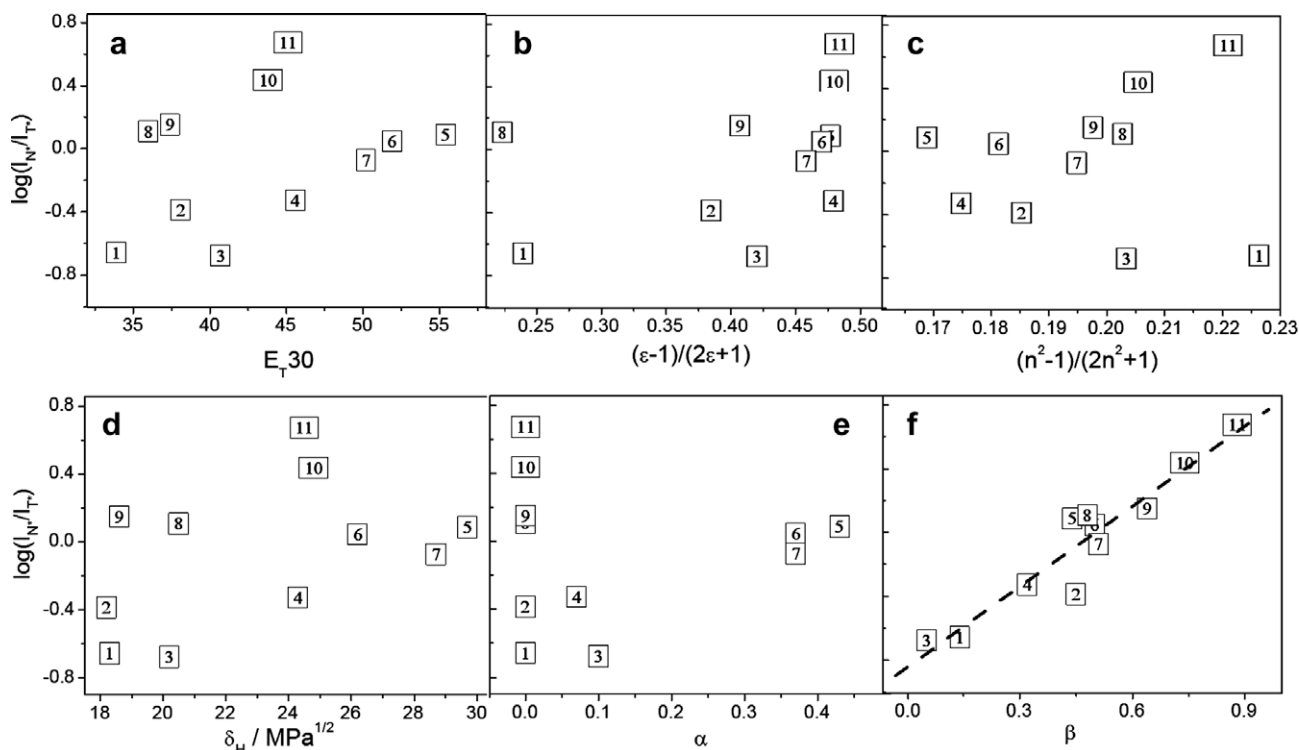


Figure 4. Dependence of $\log(I_{N^*}/I_{T^*})$ of dye **2c** on the solvent E_T30 polarity index (a), polarity $(\epsilon - 1)/(2\epsilon + 1)$ (b), and polarizability $(n^2 - 1)/(2n^2 + 1)$ (c) functions, Hildebrand's solubility parameter δ_H (d),³⁰ Abraham's hydrogen bond donor acidity α (e) and hydrogen bond acceptor basicity parameter β (f).³¹ Numbering of solvents (1–5) is as in Table 1. Additional solvents: 6-ethanol, 7-n-butanol, 8-dioxane, 9-THF, 10-DMF, and 11-DMSO. The I_{N^*}/I_{T^*} data for methanol and ethanol solutions were corrected (by a factor of 2 and 1.7, respectively) to compensate for the increased bandwidth of the T^* band.

Table 2

Time-resolved fluorescence parameters of **2a** in organic solvents

Solvent	I_{N^*}/I_{T^*}	τ_1^a , ns (α_1)		τ_2 , ns (α_2)	
		N^*	T^*	N^*	T^*
DMSO	1.47	2.21 (0.995)	2.28 (−0.46)	6.05 (0.005)	5.24 (0.54)
DMF	0.71	0.83 (0.995)	0.86 (−0.46)	5.06 (0.005)	4.83 (0.54)
MeCN	0.12	0.12 (0.998)	0.13 (−0.48)	4.99 (0.002)	5.39 (0.52)
MeOH	1.31	0.83 (0.99)	0.81 (−0.49)	5.20 (0.01)	5.30 (0.51)

^a I_{N^*}/I_{T^*} is the ratio of emission intensities of the N^* and T^* forms; τ_1 , τ_2 (ns) are the short-lived and long-lived decay times, respectively, and α_1 , α_2 are their relative amplitudes.

facilitate their applications for ratiometric measurements and fluorescence microscopy imaging.

4. Experimental

4.1. Materials and methods

All reagents were purchased from Sigma-Aldrich. Solvents for synthesis were of reagent quality and appropriately dried if necessary. For absorption and fluorescence studies, the solvents were of spectroscopic grade. Melting points were determined on a 'VEB Analytik', Dresden hostage microscope melting point apparatus, and were uncorrected. Proton NMR spectra were recorded on a Varian Mercury—400 MHz spectrometer. Tetramethylsilane (TMS) was used as an internal standard in $CDCl_3$ or $DMSO-d_6$. Mass spectra were measured with a Mass Spectrometer Mariner System 5155.

Absorption spectra were recorded on a Cary 4 spectrophotometer (Varian) and emission spectra on a FluoroMax 3.0 (Jobin Yvon,

Horiba) spectrofluorimeter at room temperature. In case of a structured emission spectrum, we selected the highest peak to determine the position of the maximum emission wavelength. Fluorescence quantum yields ϕ were determined with quinine sulfate in 0.5 M sulfuric acid ($\phi = 0.577$) as a reference,³⁵ and for **2** with 4'-(N,N-diethylamino)-3-hydroxyflavone in ethanol ($\phi = 0.51$).³⁶ All measurements were carried out in a temperature-controlled cell at 20 ± 0.1 °C. Time-resolved fluorescence measurements were performed with the time-correlated, single-photon counting technique using the frequency tripled output of a Ti-Sapphire laser (Tsunami, Spectra Physics), pumped by a Millennia X laser (Tsunami, Spectra Physics).¹¹ The excitation wavelength was set at 320 nm. The fluorescence decays were collected at the magic angle (54.7°) of the emission polarizer. The single-photon events were detected with a microchannel plate Hamamatsu R3809U photomultiplier coupled to a Philips 6954 pulse preamplifier and recorded on a multichannel analyzer (Ortec 7100) calibrated at 25.5 ps/channel. The instrumental response function was recorded with a polished aluminum reflector, and its full-width at half-maximum was 50 ps. The time-resolved decays were analyzed both by the iterative reconvolution method and the Maximum Entropy Method (MEM).³⁷ The goodness of the fit was evaluated from the χ^2 values, the plots of the residuals and the autocorrelation function.

4.2. Synthesis

Synthesis (Scheme 1) and purification of the dyes **1a–c** and **2a–c** were performed as previously described.²³ The general procedure for the synthesis of 3HBQs is described for compound **2c**.

Preparation of 4c. To a solution of 2-acetylbenzofuran (3.20 g, 20 mmol) in 50 ml mixture of dry dioxane and diethyl ether (5:1 in v/v) with 2–4 drops of 48% hydrobromic acid, 3.84 g (24 mmol) of bromine was slowly added at 0 °C up to the formation of **4c** (TLC-control). The solution was stirred at room temperature for another 30 min. Then the liquor were poured into 50 ml of ice water to afford white needle crystals of 1-(1-benzofuran-2-yl)-2-bromoethanone **4c** (4.16 g, yield 87%), pure enough for the next step.

Preparation of 3c. To a solution of 3-amino-2-naphthoic acid (2.81 g, 15 mmol) in 20 ml of DMF, 2.48 g (18 mmol) of potassium carbonate were added. The mixture was heated to 70 °C and stirred for 1 h. After cooling to room temperature, 3.11 g (13 mmol) of 1-(1-benzofuran-2-yl)-2-bromoethanone were added. Then the mixture was heated to 50 °C and stirred for 1 h. After that, the mixture was poured into 50 ml of ice water. The filtered precipitate after washing with water and drying afforded white powder of 2-(1-benzofuran-2-yl)-2-oxoethyl-3-amino-2-naphthoate **4.08 g**, which was recrystallized from ethanol. Yield: 91%.

Preparation of 2c. The 2-(1-benzofuran-2-yl)-2-oxoethyl-3-amino-2-naphthoate (0.52 g, 1.5 mmol) was added to 3.3 g of polyphosphoric acid and stirred at 120° for 2 h. After that, the mixture was poured into 10 g of ice and neutralized by 10% aqueous sodium carbonate. Filtered precipitate after washing, drying and recrystallization from DMF afforded the dark purple needles of dye **2c**, 0.38 g. Yield: 73%.

3-Hydroxy-2-(2-phenylbenzo[g]quinolin-4(1H)-one (2a): mp 237–238 °C, $\epsilon_{\max} = 7600 \text{ l mol}^{-1} \text{ cm}^{-1}$ (acetonitrile). ¹H NMR (400 MHz, DMSO-*d*₆) δ 11.55 (br s, 1H, NH), 8.86 (br s, 1H, OH), 8.79 (s, 1H, H-5); 8.15 (d, *J* = 8.9 Hz, 1H, H-6), 7.96–7.85 (m, 4H, ArH, Ar'-H'), 7.61–7.50 (m, 4H, Ar'H), 7.41 (t, *J* = 8 Hz, 1H, H-8), *m/z* (Int,%): 294 [M+1]⁺ (100).

3-Hydroxy-2-(2-thienyl)benzo[g]quinolin-4(1H)-one (2b): mp 254–255 °C, $\epsilon_{\max} = 7100 \text{ l mol}^{-1} \text{ cm}^{-1}$ (acetonitrile). ¹H NMR (400 MHz, DMSO-*d*₆) δ 11.48 (br s, 1H, NH), 8.75 (s, 1H, H-5), 8.21 (d, *J* = 8.7 Hz, 1H, H-6), 8.24 (d, *J* = 8.4 Hz, 1H, H-4'); 7.91 (d, *J* = 7.9 Hz, 1H, H-3'); 7.89–7.77 (m, 2H, H-9, H5'); 7.45 (t,

J = 8.1 Hz, 1H, H-8); 7.36 (t, *J* = 8.8 Hz, 1H, H-7); 7.27 (s, 1H, H-10), *m/z* (Int,%): 288 [M+1]⁺ (100).

1-Benzofuran-2-yl-3-hydroxybenzo[g]quinolin-4(1H)-one (2c): mp 291–293 °C, $\epsilon_{\max} = 7700 \text{ l mol}^{-1} \text{ cm}^{-1}$ (acetonitrile). ¹H NMR (400 MHz, DMSO-*d*₆) δ 11.45 (br s, 1H, NH); 8.81 (s, 1H, H-5); 8.45 (s, 1H, H-3'); 8.04 (d, *J* = 9.4 Hz, 1H, H-6); 7.92 (m, 2H, H-9,5'); 7.76 (d, *J* = 8.8 Hz, 1H, H-7'); 7.72 (d, *J* = 8.5 Hz, 1H, H-4'); 7.51 (d, *J* = 9.1 Hz, 1H, H-7); 7.42 (m, 2H, H-6',10); 7.35 (t, *J* = 8.6 Hz, 1H, H-8), *m/z* (Int,%): 328 [M+1]⁺ (100).

Acknowledgments

This work was supported by the ECO-NET and ARCUS program from the French Ministère des Affaires Étrangères between France, Ukraine, and Russia. D.A.Y. and V.V.S. are recipients of a high-level Eiffel Fellowship. V.G.P. was supported by a fellowship from University Louis Pasteur.

References and notes

- Giuliano, K. A.; Post, P. L.; Hahn, K. M.; Taylor, D. L. *Ann. Rev. Biophys. Biomol. Struct.* **1995**, *24*, 405–434.
- Kasha, M. J. *Chem. Soc., Faraday Trans.* **1986**, *82*, 2379–2392.
- Le Gourrierc, D.; Ormson, S. M.; Brown, R. G. *Progr. React. Kinet.* **1994**, *19*, 211–275.
- Formosinho, S.; Arnaut, L. J. *Photochem. Photobiol. A* **1993**, *75*, 21–48.
- Klymchenko, A. S.; Duportail, G.; Oztürk, T.; Pivovarenko, V. G.; Mély, Y.; Demchenko, A. P. *Chem. Biol.* **2002**, *9*, 1199–1208.
- Klymchenko, A. S.; Pivovarenko, V. G.; Oztürk, T.; Demchenko, A. P. *New J. Chem.* **2003**, *27*, 1336–1343.
- Shynkar, V. V.; Mély, Y.; Duportail, G.; Piémont, E.; Klymchenko, A. S.; Demchenko, A. P. *J. Phys. Chem. A* **2003**, *107*, 9522–9529.
- Shynkar, V. V.; Klymchenko, A. S.; Kunzelmann, C.; Duportail, G.; Muller, C. D.; Demchenko, A. P.; Freyssinet, J.-M.; Mély, Y. *J. Am. Chem. Soc.* **2007**, *129*, 2187–2193.
- Enander, K.; Choulier, L.; Olsson, A.; Yushchenko, D. A.; Kanmert, D.; Klymchenko, A. S.; Demchenko, A. P.; Mély, Y.; Altschuh, D. *Bioconjugate Chem.* **2008**, *19*, 1864–1870.
- Shvadchak, V. V.; Klymchenko, A. S.; De Rocquigny, H.; Mély, Y. *Nucleic Acids Res.* **2009**, doi:10.1093/nar/gkn1083.
- Sytnik, A.; Gormin, D.; Kasha, M. *Proc. Natl. Acad. Sci. U.S.A.* **1994**, *91*, 11968–11972.
- Roshal, A.; Grigorovich, A.; Doroshenko, A.; Pivovarenko, V. G.; Demchenko, A. P. *J. Phys. Chem. A* **1998**, *102*, 5907–5914.
- Poteau, X.; Saroja, G.; Spies, C.; Brown, R. J. *Photochem. Photobiol. A* **2004**, *162*, 431–439.
- Yushchenko, D. A.; Vadzyuk, O.; Kosterin, S.; Duportail, G.; Mély, Y.; Pivovarenko, V. G. *Anal. Biochem.* **2007**, *369*, 218–225.
- Yushchenko, D. A.; Shvadchak, V. V.; Klymchenko, A. S.; Duportail, G.; Mély, Y.; Pivovarenko, V. G. *New J. Chem.* **2006**, *30*, 774–781.
- Gao, F.; Johnson, K.; Schlenoff, J. J. *Chem. Soc., Perkin Trans. 2* **1996**, 269–273.
- Yushchenko, D. A.; Bilokin, M. D.; Pivovarenko, O. V.; Duportail, G.; Mély, Y.; Pivovarenko, V. G. *Tetrahedron Lett.* **2006**, *47*, 905–908.
- Yushchenko, D. A.; Shvadchak, V. V.; Klymchenko, A. S.; Duportail, G.; Pivovarenko, V. G.; Mély, Y. *J. Phys. Chem. A* **2007**, *111*, 8986–8992.
- Yushchenko, D. A.; Shvadchak, V. V.; Bilokin, M. D.; Klymchenko, A. S.; Duportail, G.; Mély, Y.; Pivovarenko, V. G. *Photochem. Photobiol. Sci.* **2006**, *5*, 1038–1044.
- Bilokin, M. D.; Shvadchak, V. V.; Yushchenko, D. A.; Duportail, G.; Mély, Y.; Pivovarenko, V. G. *J. Fluorescence* **2009**, *19*, 545–553.
- M'Baye, G.; Klymchenko, A. S.; Yushchenko, D. A.; Shvadchak, V. V.; Oztürk, T.; Mély, Y.; Duportail, G. *Photochem. Photobiol. Sci.* **2007**, *6*, 71–76.
- Abboud, J.-L. M.; Notario, R. *Pure Appl. Chem.* **1999**, *71*, 645–718.
- Abraham, M. *Chem. Soc. Rev.* **1993**, *22*, 73–83.

32. Yushchenko, D. A.; Shvadchak, V. V.; Klymchenko, A. S.; Duportail, G.; Pivovarenko, V. G.; Mély, Y. *J. Phys. Chem.* **2007**, *111*, 8986–8992.
33. Laws, W.; Brand, L. *J. Phys. Chem.* **1979**, *83*, 795–802.
34. Bader, A.; Pivovarenko, V. G.; Demchenko, A. P.; Ariese, F.; Gooijer, C. *J. Phys. Chem. B* **2004**, *108*, 10589–10595.
35. Eastman, J. W. *Photochem. Photobiol.* **1967**, *6*, 55–72.
36. Chou, P.; Martinez, M.; Clements, J. *J. Phys. Chem.* **1993**, *97*, 2618–2622.
37. Livesey, A.; Brochon, J. *Biophys. J.* **1987**, *52*, 693–706.